



## 1. INTRODUCTION

Centrifugal pumps are one of the most useful machines in a wide variety of industrial systems for fluid transportation. Optimal design or optimization of these machines for reducing the energy consumption and improving the performance has been receiving a great attention from researchers.

Pump design is normally based on Euler's 1D theory in which some ideal assumptions like infinite number of blades and zero thicknesses for them are assumed. Fluid mechanic theories help designers to size the preliminary dimensions of the machine i.e. inlet and outlet diameter of the impeller and the blade angles to ensure the required head in a specific mass flow rate (Gülich, 2008; Karrasik *et al.*, 2012). Experimental studies and the designer's experiences help to modify this ideal preliminary design for the real machines by considering loss mechanisms, fluid behavior, manufacturing and mechanical considerations (Nourbakhsh *et al.*, 2007). The design in this stage is modified by adding some details about blade curvatures, blade thicknesses and angles (Fu *et al.*, 2018) and also some features i.e. splitter characteristics. After that, the computational fluid dynamic tools could be used to evaluate or improve the machine characteristics to obtain the acceptable performance (Mojaddam and Torshizi, 2017) to complete the design procedure.

Many researchers have analyzed the pump characteristics numerically and experimentally. Wang *et al.* numerically simulated a multi-stage centrifugal pump and provided guidance for optimization of these machines through testing a prototype (Wang *et al.*, 2017). Despite the proved advantages of splitter blades in the performance of the centrifugal pumps and compressors during past years (Miyamoto *et al.*, 1992; Moussavi *et al.*, 2017), their optimal design and optimization have received less attention in the literature. Kergourlay *et al.* (2007) studied the effect of adding splitter blades on velocity and pressure fields of a centrifugal pump in different flow rates numerically and experimentally. They concluded that the splitters could decrease the pressure fluctuations. Gölcü *et al.* (2006) studied the effect of splitter blades length on a centrifugal pump performance. Their experimental results showed that an impeller with splitter blades with 80% length of the full blades saved 6.6% energy and resulted in 1.14% improvement in efficiency. Li *et al.* (2006) investigated the effect of splitter blades on the reverse flow patterns on a centrifugal pump blade in their investigation. They showed the splitter blades is utilized to control the reverse flow. They also concluded that the pump head improvement was due to splitter blades.

Shigemitsu *et al.* (2013) studied the effect of splitter blades on performance of mini-centrifugal pumps. Their experimental data declared that the low-velocity zone between two blades is removed because of splitter blades. Korkmaz *et al.* (2017) studied the effect of different parameters on Deep

Well Pumps (DWP) performance such as the number of blades, the blade discharge angles, and the splitter blade lengths by experimental tests.

Several researches implemented the optimization techniques on pump components especially on the impeller. Optimization methods can be categorized into three main groups. First, the gradient-based methods in which the gradient of the goal function is calculated and the local optimized points are found. Second, the exploratory methods like Genetics Algorithm (GA) and Simulating Annealing, which are based on evolution theory and are capable of finding the optimized point through the entire domain. Calculation expenses are the weakness of these methods. Finally, the function approximation methods like Design of Experiment (DoE) and Neural Network (NN) techniques in which an approximated relation between the input parameters and the desired outcomes is found. These methods could decrease the optimization steps significantly (Shahpar, 2000). The optimization method should be selected carefully based on the nature of the problem and ignoring the fluid physics would lead to malfunction.

Lian and Lio (2005) introduced a multi objective optimization method using Response Surface Method (RSM) and GA. They used Latin Hypercube Design (LHD) method to construct the design space. In their research, a single-stage pump design is optimized via 11 design variables including meridional geometry and blade angles. Safikhani *et al.* (2011) used NN and GA to perform a multi-objective optimization on a centrifugal pump. Blade camber line was parameterized using simple Bezier curve in order to control the optimization parameters. Efficiency and NPSH were the objectives of their optimization process. Kim *et al.* (2011) optimized a mixed-flow pump considering a fixed meridional shape. The optimization parameters were geometry of the impeller and the diffuser. They used the full-factorial technique of DoE to determine the design space and the RSM for finding the optimized operating point. Derakhshan *et al.* (2013) optimized a centrifugal pump blade using NN and an artificial bee colony algorithm. The results showed 3.59% improvement in efficiency and 6.89m increase in the total head. Bellary *et al.* (2014) selected inlet and outlet angle of the blade of a centrifugal pump as the optimization parameters and used a 3D Navier-Stokes solver to optimize the geometry of the blade in order to improve the hydraulic efficiency. Huang *et al.* (2015) used GA in order to optimize the impeller loading using ten selected parameters on meridional contours. Zhang *et al.* (2017) introduced a novel optimization method for the multiphase pump impeller based on the GA and boundary vortex flux by varying the impeller geometry. Pei *et al.* (2016) used the combination of DoE, RSM and GA on the meridional plane of a centrifugal pump impeller.

DoE as a promising optimization technique has been widely implemented in turbomachines. Many different turbomachines such as compressors (Samad *et al.* 2008, Mojaddam and Pullen, 2019),

turbines (Hatami *et al.*, 2015) and fans have been optimized using DoE techniques. Bonaiuti *et al.* (2002) optimized the performance of a transonic centrifugal compressor impeller by adopting geometrical parameters consisting of the number of blades, inlet hub and shroud diameters, outlet blade height, impeller axial length, and blade inlet leading angle, using DoE. Pie *et al.* (2017) utilized an orthogonal DoE technique to study the effect of impeller inlet diameter, inlet incidence angle, and blade wrap angle on the cavitation characteristics of a centrifugal pump. The optimized case accomplished a better hydraulic and cavitation performance. Meanwhile, the NPSHR decreased by 0.63m in comparison with the original case. Suh *et al.* (2017) used a central composite design technique of DoE and a hybrid multi-objective evolutionary algorithm coupled with a surrogate model to optimize the second stage of a multiphase pump. Their results showed hydraulic performance improvement.

In the mentioned researches in pump performance optimization, the effect of splitter blade parameters on the pump performance has not been investigated comprehensively. Hence, implementing the design of experiment technique to reduce the optimization steps for exploring several parameter effects is the main objective of this article.

In the present study, investigating the effects of splitter blades on the pump performance is performed in two stages. In the first stage, two impellers are manufactured and experimentally tested by adding the splitter blades to the original impeller which has 6 main blades and no splitter. The new impellers have the splitters by the length of one-third and two-third of the main blade length, respectively. The case with the best performance is considered for the optimization in the next stage. Different parameters are chosen for the optimization process using DoE in the second stage. They are the main and the splitter blade leading edge position and the location of splitters in the passage. Overall efficiency and total head of the pump are considered as the objective functions for finding the optimal geometry.

## 2. METHODOLOGY

### 2.1. Design Space

DoE can be defined as the combination of statistical and mathematical methods and due to its simplicity and acceptable accuracy, has attracted researchers' attention in optimization problems (Montgomery, 2017). DoE technique introduces statistical tools to form a design space around the initial values of the design parameters. The ability of DoE to study the effect of independent parameters on the objective functions makes it useful in many engineering applications.

Full factorial, Box-Behnken, central composite design (CCD), and Taguchi are the main techniques of the DoE for design space generation. Computation cost and the type of the problem suggest the suitable technique for the problem. The

full factorial technique searches all of the design space. By increasing the levels of parameters this technique is not efficient and generates numerous design space points. However in the other techniques, there is no need to search all possible points and it helps to decrease the computational cost by having acceptable accuracy (Mojaddam and Pullen, 2019). Box-Behnken technique makes an efficient design space in which only a portion of full factorial points are necessary to construct for investigating the second-order effect of parameters.

Creating the design space points by Box-Behnken technique for a problem with three parameters varying at three levels which are named, -1, 0 and 1 is shown in Fig. 1. Each point of designed experiments suggests a combination of three parameters. For this problem, an imaginary cube around the central point (means all parameter at their 0 level) suggests the black points on the cube edges as the design space. The design points, in fact are lying on a sphere of radius  $\sqrt{2}$  (Montgomery, 2017). This design does not include the cube vertices (unlike the CCD design technique), which can be advantageous when these points are impossible to examine based on the problem constraints.

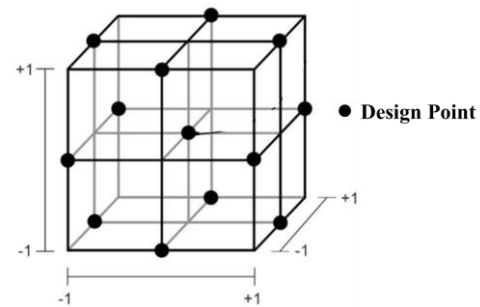


Fig. 1. Box-Behnken design space.

### 2.2. Response Surface Method

Evaluating the effect of design space points on the objective functions could be handled using Response Surface Method (RSM). This method includes mathematical or statistical techniques to analyze the problems in which the objective, called response, is influenced by many parameters (Montgomery, 2017). It approximates the relation between the design parameters and response by surface fitting to optimize the objective or response.

Each design point is related to one objective function,  $y$ , which is derived from  $k$ -tuple  $(x_1, \dots, x_k)$  in which the  $x_i$  is each parameter values for  $k$  parameters. A second order polynomial curve can be fitted to the design space using Eq. (1) (Myers *et al.*, 2016).

$$y = \beta_0 + \sum_{i=1}^k \beta_i x_i + \sum_{i=1}^k \beta_{ii} x_i^2 + \sum_{i < j} \beta_{ij} x_i x_j + \varepsilon_i \quad (1)$$

In which  $\beta$ s are the unknown coefficients and  $\varepsilon$  is the deviation of the fitted values from the real data.

Least square method (LSM) is used to find  $\beta$ s by minimizing the errors ( $\epsilon_i$ ) using the following equation (Eq. (2)), (Myers *et al.*, 2016).

$$L = \sum_{i=1}^k \epsilon_i^2 \quad (2)$$

### 2.3. Optimization Procedure

In this article the most important parameters in splitter blade geometry are recognized and the boundaries of these parameter values are properly defined to construct the problem design space based on the Box-Behnken method. The CFD is used for deriving the flow characteristics for each design space geometry. Overall efficiency and total head of pump are considered as the objectives. The response surface for the objectives are obtained using RSM and the approximated functions are optimized using GA method (Talebian and Mojaddam, 2017). The optimized points are evaluated using CFD and the flow behavior features are compared to the original geometry. The step by step procedure can be omitted is shown in Fig. 2.

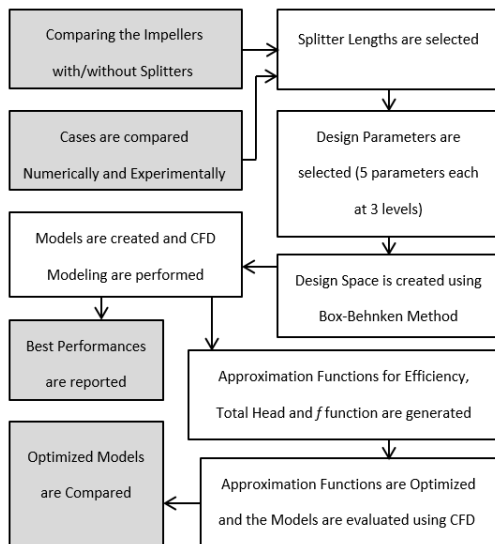


Fig. 2. Optimization process in this research.

### 3. TEST CASES

The under-study pump is a single stage centrifugal pump. The impeller outlet diameter and its width are 209mm and 17mm, respectively with 27.5° blade outlet angle. The design point flow rate is 55 m<sup>3</sup>/hr at 1450 rpm rotational speed with 26.8 specific speed in SI unit (equal to 1348 in US unit).

Figure 3, shows the meridional view of all three impellers. Case I is the 6-bladed impeller without splitters. Case II and III are impellers with splitters by the length of 33% and 66% of the main blade

length, respectively which were designed and fabricated for this study.

All impellers are fabricated, installed and tested in the research and development test cell in which the performances are driven under steady state condition.

Pneumatic butterfly valves are used to adjust the flow rate. Pressures are measured by strain gauges at the pump inlet and outlet. An electromagnetic flow meter is installed to measure the flow rate at the pump outlet. Figure 4 shows the test cell, the schematic of the test cycle and the original impeller (Ehghaghi *et al.*, 2017).

The pump generating head is obtained through pressure measurement at the suction and discharge of the pump.

The ratio of water power to pump shaft power is used for calculating the overall efficiency (Eq. (3)), (Karassik *et al.*, 2001).

$$\eta = \gamma QH / \dot{W} \quad (3)$$

Where  $\gamma$ , Q, H are the flow specific weight, the volumetric flow rate and the pump total head, respectively.  $\dot{W}$  is the brake horse power which is the available power at the pump shaft and is calculated using electromotor measured power, its efficiency and the mechanical efficiency. The product of these two efficiencies is considered constant and equals to 83%.

### 4. NUMERICAL MODEL

Using the geometry of pump parts, including the impeller and the volute, the pump is modeled. Unstructured tetrahedral grids with prismatic boundary layer meshes are used for the whole domain for three different cases. Figure 5 shows the grids for the impeller and the volute of case I.

Five layers of grids with 1.2 growth rate are considered near the wall surfaces and the first grid thickness is properly adjusted in the moving and stationary domains for having  $y^+$  in the range of 10. Tip clearance is considered for the impeller in the mesh generation and it is 0.8mm constant along the impeller shroud.

Mesh independency analysis on the impeller torque proves that at least about 4.1 million grids for whole model are adequate to achieve reliable results as shown in Fig. 6.

The mesh aspect ratio quality average is 0.85, expansion factor is limited to 12 and the minimum angle in the worst case is not less than 38 degrees.

A three dimensional viscous solver is used and the RANS equations are solved iteratively in which momentum equations are discretized using the second-order upwind method. Steady state

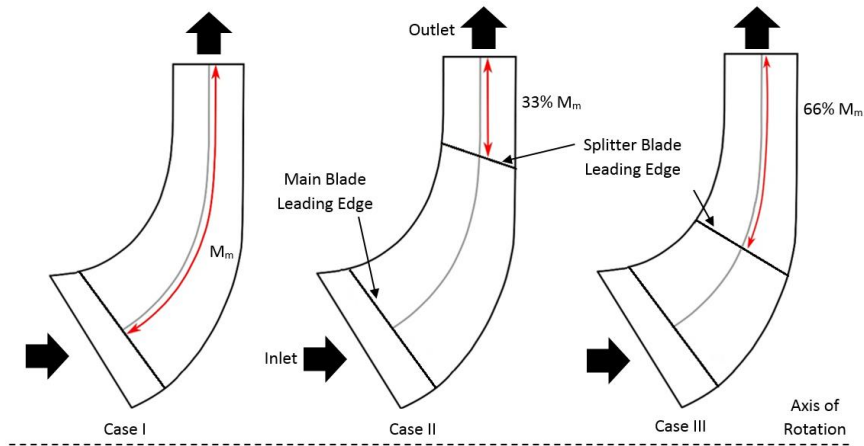


Fig. 3. Meridional view of cases I, II and III.

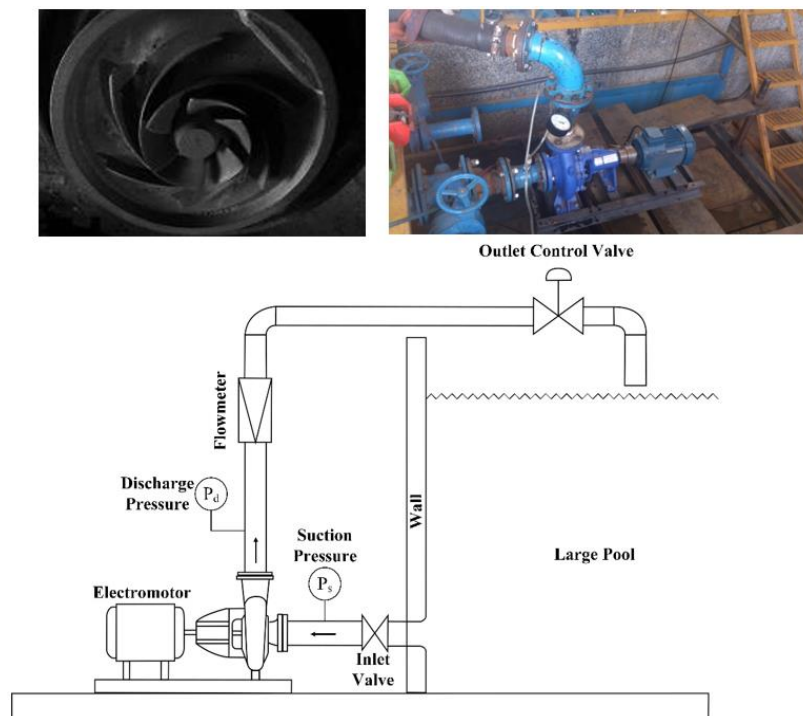


Fig. 4. Impeller cast model, test rig and the schematic.

condition with constant density is considered (Mojaddam *et al.*, 2015).

A frozen rotor method is used to properly handle the interface between rotating impeller and the stationary parts. Shear-stress transport (SST) turbulence model is used for treating the Reynolds stress terms in the momentum equations in order to accurately model the turbulence at both near-wall and far field regions using  $k-\omega$  and  $k-\epsilon$  models respectively. Total pressure at the impeller inlet and the mass flow rate at volute outlet are considered as the inlet and outlet boundary conditions. Convergence is testified by reaching the residuals to the order of  $1E-5$  and the stability of impeller torque value.

## 5. RESULTS AND DISCUSSION

Pump total head and overall efficiency are used in order to validate the numerical results. Using numerical results, the weighted average of the head at the inlet (suction) and the outlet (discharge) sections (Mojaddam *et al.*, 2012) are used to calculate the pump total head via the following relation, Eq. (4), in which,  $d\dot{m}$ , is the mass flow rate through each mesh element at the suction or at the discharge and  $\dot{m}$  is the pump mass flow rate.

$$H = \frac{\sum p_D d\dot{m} - \sum p_S d\dot{m}}{\dot{m} \gamma} \quad (4)$$

Overall efficiency is then calculated using Eq. (5) in which  $\tau$  and  $\omega$  are the impeller calculated torque and impeller rotational speed, respectively.

$$\eta = \frac{\dot{m}gh}{\tau\omega} \quad (5)$$

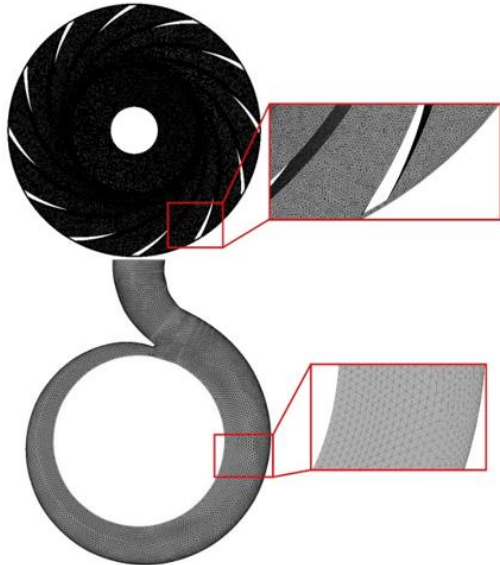


Fig. 5. Impeller and volute grids for Case I.

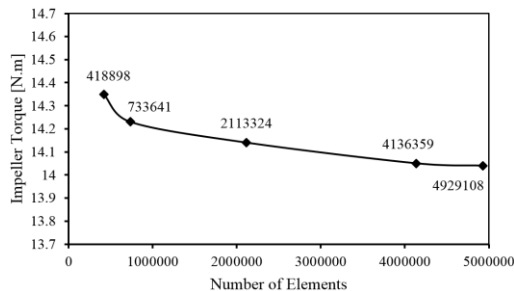


Fig. 6. Mesh independency study.

### 5.1. Validation

Three case models are validated through experimental data in different mass flow rates at the design point rotational speed. Pump total head versus volumetric flow rate is reported in this regards as shown in Fig. 7. The uncertainty analysis for head and efficiency are calculated using Eq. (6) (Beckwith *et al.*, 2009).

$$W_R = \left[ \left( \frac{\partial R}{\partial x_1} W_1 \right)^2 + \left( \frac{\partial R}{\partial x_2} W_2 \right)^2 + \dots + \left( \frac{\partial R}{\partial x_n} W_n \right)^2 \right]^{\frac{1}{2}} \quad (6)$$

In which  $W_R$  is the uncertainty of  $R$  and this variable is affected by  $x_1, \dots, x_n$  parameters.  $W_i$  are the associated errors in measuring each  $x_i$ . In this study, the uncertainty analysis shows 0.76% and 3.3% error for total head and overall efficiency, respectively.

Numerical results are in a satisfactory agreement with experimental data, especially around the

design point where the flow rate is 55 m<sup>3</sup>/hr. Around BEP the differences between experimental and numerical results do not exceed 4% which occurs for case II. With mass flow rate decrease, the amount of the error increases and that is due to the leakage flow through the gap between volute and the impeller that is not considered in numerical simulation.

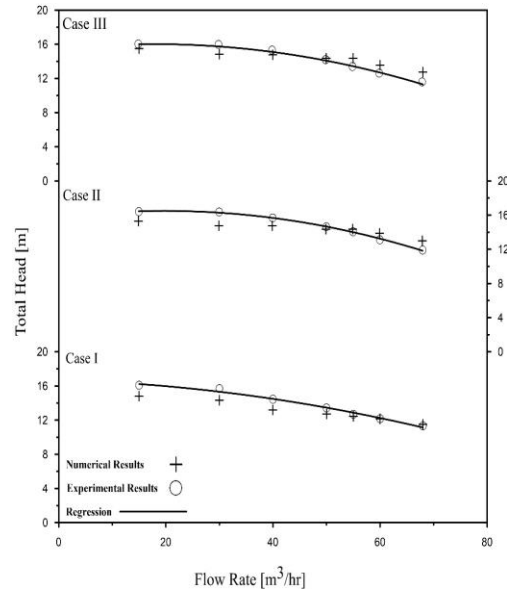


Fig. 7. Experimental and numerical results.

The maximum deviation in efficiency is limited to 4.54% for case I. The deviations between experimental and numerical results can be due to numerous reasons i.e. the differences between the actual geometry and the model, the leakages, heat transfer, roughness effect (Mojaddam *et al.*, 2012), disk friction and all mechanical losses which are not considered in model and also the experimental errors (Nikparto and Schobeiri, 2017) in parameter measurements. Experimental and numerical results are shown and compared in Table 1 around BEP.

### 5.2. Splitter Blades

Experimental results for cases I, II and III are shown in Fig. 8. Pump total head and efficiency versus flow rate are reported for all cases simultaneously. Pump total head improvement is obvious in case of using splitters. Using longer splitter blades (Case III) results in the highest total head among the cases.

Use of splitter blades on the impeller leads to a head increase especially in the higher flow rates. Better fluid guidance by the blades can be considered for this improvement which forces the fluid to follow the blade profile near the impeller outlet. This leads to a decrease in slip and an increase in slip factor (Kergourlay *et al.*, 2007; Memardefzouli *et al.*, 2009). The efficiency of all cases guarantees the negligible effect of splitter blades in this regard. Near the design point, leakage and shock losses decrease and because of this, head increases more noticeably around this point. Figure 9 shows the

**Table 1 Experimental and numerical results for cases**

	Case I		Case II		Case III	
	$\eta$ [%]	$H$ [m]	$\eta$ [%]	$H$ [m]	$\eta$ [%]	$H$ [m]
Experimental	79.16	12.67	78.55	13.36	80.02	14.01
Numerical	82.76	12.46	81.97	13.9	82.04	14.41
Deviation [%]	4.54	1.69	4.35	3.99	2.5	2.81

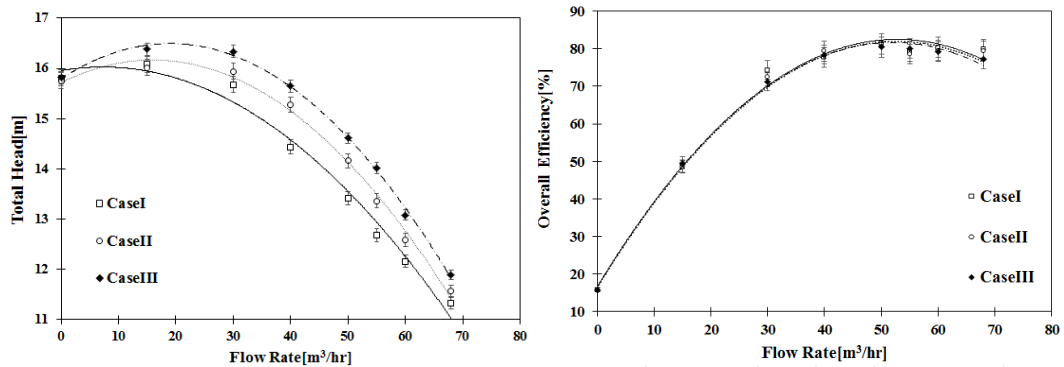


**Fig. 8. Experimental results comparison for all three cases.**

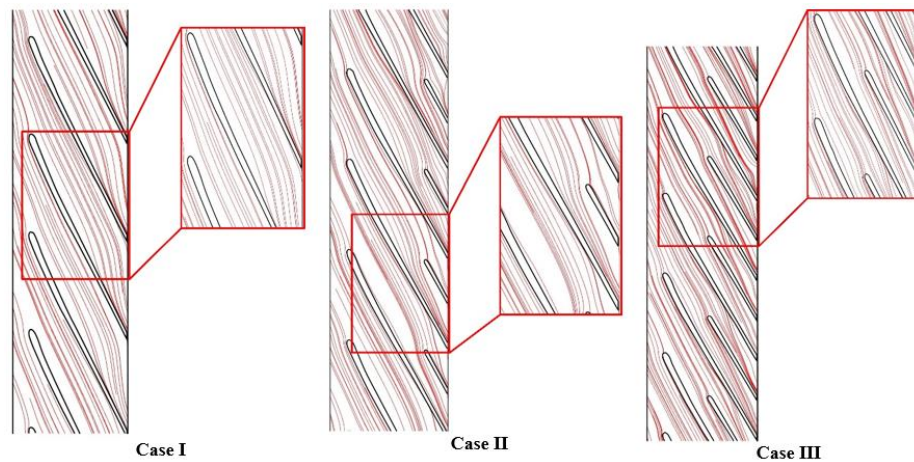


**Fig. 9. Streamlines Between Blades.**

streamlines between blades in all three cases. Better fluid guidance and higher velocities are obvious in Case II and III in comparison with Case I due to the splitters presence. In Case II, due to shorter splitters in comparison with Case III, the fluid flow is not guided properly and as it can be seen, the splitter blade effect is major at the impeller outlet.

### 5.3. Optimization

For investigating the effect of the splitter and the main blade inlet shape on the pump performance, case III is used as the starting geometry as it showed better performance in comparison with the other cases. Five parameters have been considered

and the effects of them on pump total head and efficiency are investigated. Figure 10 shows the optimization parameters. P1 and P3 adjust the splitter blade leading edge while P2 and P4 are considered for the main blade leading edge position. P5 is the position of splitters between blades. As there are six blades, the circumferential angle between two succeeding blade is  $\alpha = 60$  degree. For handling the position of splitters between blades, the boundaries are specified in a way that the splitter moves from middle section toward the suction side or pressure side of the main blades by 10% as show in Fig. 10.

The upper and lower boundaries of the parameter

variations are specified upon percentage of their length of the hub and shroud curves and tabulated in Table 2.

Box-Behnken technique is used to construct DoE design space. This method with 5 parameters, each at three levels, results in the total number of 46 design points. As it was mentioned, this technique reduces the number of required experiments noticeably to identify the best case while the algorithm like full factorial, required  $3^5$  design points in this problem (Montgomery *et al.*, 2009).

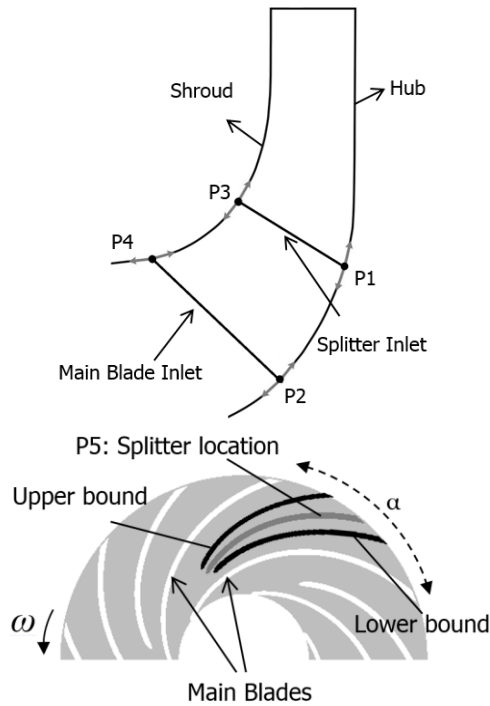


Fig. 10. Optimization parameters.

Table 2 Optimization parameters variation boundaries

Design Points	Lower Boundary	Upper Boundary
P1	56.1% $M_h$	75.9% $M_h$
P2	90% $M_h$	110% $M_h$
P3	56.1% $M_s$	75.9% $M_s$
P4	90% $M_s$	110% $M_h$
P5	-10% $\alpha$	+10% $\alpha$

All the design point geometries are constructed and modeled and solved to obtain the pump total head and overall efficiency. Figure 11 shows the results for all design points. The best performances can be captured based on Table 3 naming.

Table 3 Cases from DoE design Space

Cases	The Case with ...
Case 0	Starting Design point
Case A	Max $\eta$ in DoE Design space
Case B	Max $H$ in DoE Design space
Case C	Max $f$ in DoE Design space

The efficiency of case 0 with six splitters is 82.03% and the total head is 14.41m. After evaluation of all cases, case A shows 82.12% efficiency and case B has 15.04m total head which means total head can be improved about 4.4%. In this case, case B, head increases without sacrificing the overall efficiency.

Using Eq. (1), two approximation functions are obtained for efficiency and total head which are named  $\hat{\eta}$  and  $\hat{H}$ , respectively. For considering the efficiency and total head simultaneously, Eq. (7) is used (Asgarshamsi *et al.*, 2015). In which  $C$  is a coefficient to justify the importance of efficiency or total head for the designer which is set to 0.5 in this research. Superscript 0 stands for initial value which is the characteristics of the starting point.

$$f_i = C \left( \frac{1-\eta_i}{1-\eta_0} \right) + (1-C) \left( \frac{H_0}{H_i} \right) \quad (7)$$

Obtaining  $f$  for all design points, a second order polynomial curve is fitted using Eq. (7) and the approximation function is named,  $\hat{f}$ .

Three approximated functions clearly show the effect of parameter alteration on the outcomes. GA is used to explore the optimum for the obtained functions through all parameter bounds. The results of optimization process for each function are used to construct the model and the CFD results are analyzed to obtain the pump performance. (Table 4).

Table 4 Cases from optimizing approximation functions

Cases	The Case with ...
Case D	Max $\eta$ from Optimizing $\hat{\eta}$
Case E	Max $H$ from Optimizing $\hat{H}$
Case F	Max $f$ from Optimizing $\hat{f}$

Table 5 shows the values of total head and overall efficiency for these cases. The case with maximum total head, Case E, shows nearly the same performance in comparison with the case obtained from DoE implementation (Case B) and showed about 4.4% improvement in comparison with the initial case, Case 0. While By optimizing the approximate function for efficiency, Case D efficiency is lower than Case A and it can be considered as a drawback of response surface method and using the approximation function. Considering both factors, optimizing the approximate function, Case F, shows 0.3% less efficiency than Case 0, while total head is improved by 4.4%.

Figure 12 shows all the cases compared with the initial geometry, Case 0. It can be seen that both Case A and Case D, in which the optimizing target is overall efficiency, the positions of leading edges move toward the exit. Having shorter blades in comparison with Case 0 ensures the higher efficiency as the friction losses are decreased. By comparing the efficiency values, Case A is

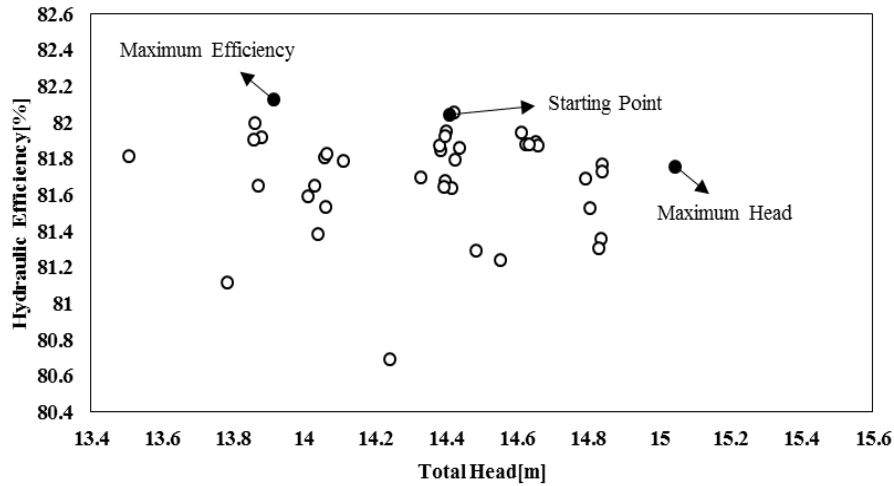


Fig. 11. Pump performance for all design points.

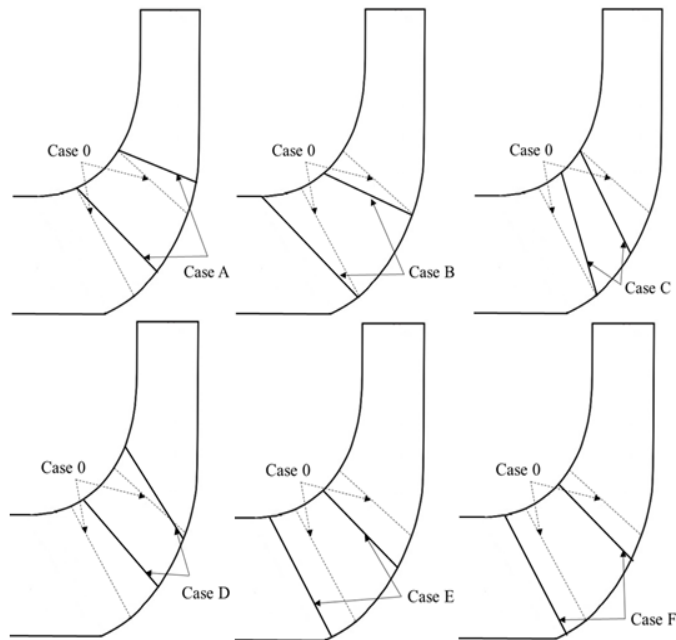


Fig. 12. Meridional view of Cases A to F in comparison to Case 0.

considered for further analysis as the model with the maximum efficiency.

Evaluating the cases with the highest head, Case B and E show that having the longer blades results in the higher total head. In Case B, the hub length of the main blade and the splitter are the same as Case 0 but at shroud, both of them are increased by 10%. Which means the ratio of splitter length to main blade length are the same in hub and shroud and the same as the original case. For Case E also the same thing can be observed. The length ratio of splitter to the main blade is equal at hub and shroud.

The variation of total head is about 11% and the efficiency variation is limited to 1.7% (refer to Fig. 11) for all design points, hence it can be seen that the effect of the under-study parameters are considerable on the total head and have negligible

effects on the efficiency. This shows that when both efficiency and total head are considered simultaneously, Case C and F, the shapes are similar to the cases with the highest total head (Case B and E).

Table 5 Impellers with maximum head, efficiency and multi-objective optimized results

Objective	Case 0	Best of DoE	Approximate function
$\eta$ [%]	82.04	Case A: 82.12	Case D: 81.78
$H$ [m]	14.41	Case B: 15.03	Case E: 15.04
$f$	$\eta$ [%]	Case C	81.71
	$H$ [m]		15.01
			Case F
			81.75
			15.04

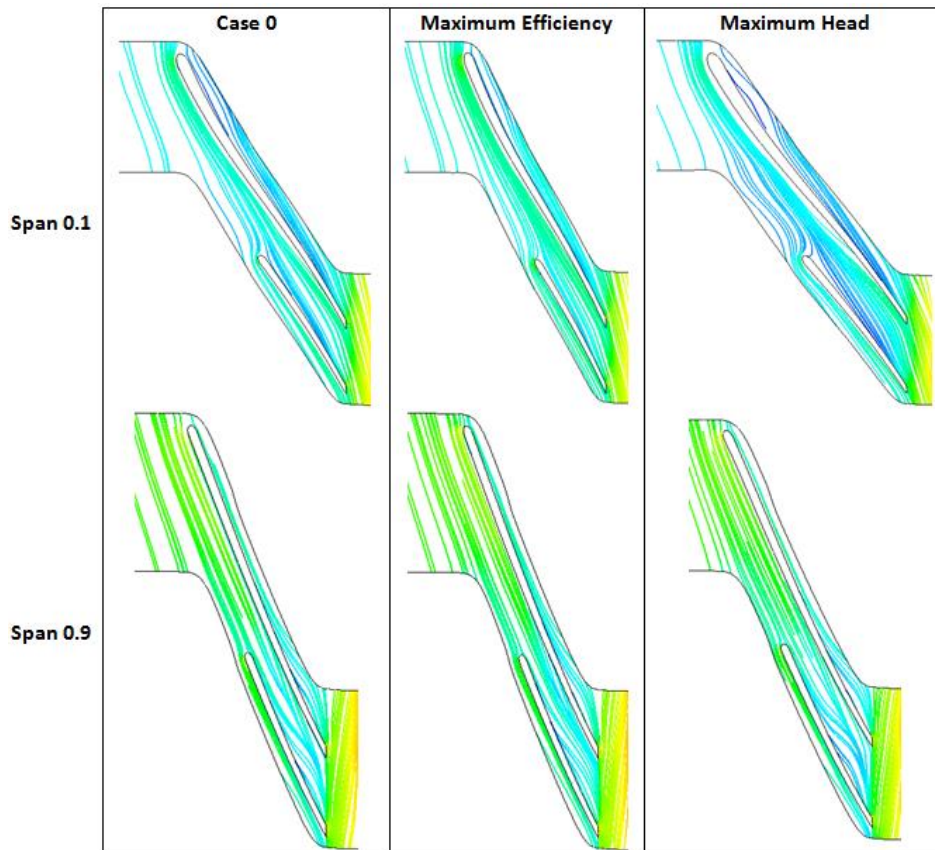


Fig. 13. Streamline near hub and near shroud spans for the optimal cases and Case 0.

The location of splitter between two successive main blades is varied by  $P5 (= a/2)$ . This parameter upper bound is defined when the splitter moves in opposite of rotational direction (-10%) and moving in the direction of the impeller rotation is considered the lower bound (+10%). The results show, the cases with the higher efficiency are those with the splitters near the lower bound of  $P5$ , which means moving the splitters in direction of impeller rotational direction results in the higher efficiency. The cases with the higher total head experience the splitter at the middle or when splitter moves toward the upper bound of  $P5$ . (The case with the highest total head has  $P5 = a/2 - 2.5\%$ )

For analyzing the flow pattern differences at different cases, Case A is considered as the case with the highest efficiency and Case E for the highest total head. The effect of shape on the flow field can be visualized by comparing the streamline at different spans of impeller passage.

Figure 13 shows the flow streamlines at near hub (span=0.1) and near the shroud one (span=0.9) for the cases with maximum efficiency (Case A) and maximum total head (Case E) and the original case in DoE procedure (Case 0).

Comparing case A with case 0 at span=0.1, shows that retarding the main blade and splitter results in better flow guidance, as the hub profile is shortened in case A. In case E, when the blade length increases, the total head is also increased however

the streamlines do not follow the blade curvature smoothly. In his configuration the efficiency is also decreased as the friction losses are increased. As it is mentioned before in the cases with the higher total head, the splitters move in the opposite direction of the impeller rotational direction. The streamlines in Fig. 13, Case E, shows that when the distance between splitter and the suction side of the main blade (in the shown blade to blade view) is increased, the flow distortion occurs which influences the overall efficiency which can be seen in both near the hub and near the shroud spans.

When streamlines at span=0.9 are considered, in all cases, the disturbances are not negligible as the impeller is un-shrouded in this study and flow circulates from the pressure side to suction side from the clearances as it can be seen at the near the shroud span. Comparing case A and Case 0 shows that their shroud profile lengths for the main blades and splitters are nearly the same (Fig. 12) hence the flow guidance in these cases are similar at the near shroud span. In case E, both main blades and splitter lengths are increased hence the flow guidance through the passage is also the same and further distortion can be considered as the result of the increased distance between splitter and suction side of its successive main blade.

## 6. CONCLUSION

Investigating the effects of splitter blades on the

pump performance is performed in this research. Three cases are considered in which case I, has no splitter and case II and III are the impellers with splitters by the length of 33% and 66% of the main blade, respectively. Case III with the best performance among three cases is considered for optimization algorithm as the base case. Different parameters are considered and using Box-Behnken technique in DoE, the design space is created. Overall efficiency and total head are considered as the objective functions separately and simultaneously. Second order polynomial curves are fitted for each function and GA is implemented on approximated functions for finding the optimum. The conclusion can be itemized as following:

- 1- By adding short splitters (Case II) to impeller without splitters (Case I), the total head increases by about 5.4% however it causes efficiency reduction as the friction losses are increased. In case (III) where the splitter lengths are two-third of the main blade length, the total head is increased by 10.6% with negligible effect of overall efficiency.
- 2- Exploring the effect of leading edge position of the main blade (P2, P4) and the splitter (P1, P3) and also the splitter location between two main blades (P5) shows that in the cases with the better performance by decreasing/ increasing the length of splitter, the length of the main blades should be decreased/ increased accordingly in such a way that the ratio is kept nearly constant.
- 3- Longer splitters results in the higher total head as the energy transfer between the blades and fluids are increased and the efficiency reduces as the friction losses are increased.
- 4- Moving the splitter in direction of impeller rotation direction increases the efficiency as it better guides the flow near the suction side of the main blades. Moving in the opposite direction results in total head increase.
- 5- The effect of studied parameters of splitters on the efficiency is so marginal, but they have significant effect on the total head. Hence when both efficiency and total head are considered simultaneously, the resulted geometry is in resemble to the cases with the highest total head.

#### ACKNOWLEDGEMENTS

The authors gratefully and respectfully acknowledge the support of CEO and staff of Navid Sahand Company in this study.

#### REFERENCES

Asgarshamsi, A., A. H. Benisi, A. Assempour and H. Pourfarzaneh (2015). Multi-objective optimization of lean and sweep angles for stator and rotor blades of an axial turbine. *Proceedings of the Institution of Mechanical*

*Engineers, Part G: Journal of aerospace engineering* 229(5), 906-916.

Beckwith, T. G., R. D. Marangoni and J. H. Lienhard (2009). *Mechanical measurements*. Addison-wesley, MA, US.

Bellary, S. A. I. and A. Samad (2014, June). Improvement of efficiency by design optimization of a centrifugal pump impeller. In *ASME Turbo Expo 2014: Turbine Technical Conference and Exposition*, Düsseldorf, Germany.

Bonaiuti, D., A. Arnone, M. Ermini and L. Baldassarre (2002, January). Analysis and optimization of transonic centrifugal compressor impellers using the design of experiments technique. In *ASME Turbo Expo: Power for Land, Sea, and Air*, Amsterdam, The Netherlands.

Derakhshan, S., M. Pourmahdavi, E. Abdollahnejad, A. Reihani and A. Ojaghi (2013). Numerical shape optimization of a centrifugal pump impeller using artificial bee colony algorithm. *Computers & Fluids* 81(Jul), 145-151.

Ehghaghi, M. B., M. Vajdi, M., Namazizadeh and M. Hajipour (2017). Experimental and numerical study of double splitter blades effect on the centrifugal pump performance. *Modares Mechanical Engineering* 17(3), 196-204.

Fu, D. C., F. J. Wang, P. J. Zhou, R. F. Xiao and Z. F. Yao (2018). Impact of Impeller Stagger Angles on Pressure Fluctuation for a Double-Suction Centrifugal Pump. *Chinese Journal of Mechanical Engineering* 31(1), 10-25.

Gölcü, M., Y. Pancar and Y. Sekmen (2006). Energy saving in a deep well pump with splitter blade. *Energy conversion and management* 47(5), 638-651.

Gulich, J. F. (2008). *Centrifugal pumps*. Springer, Berlin, Germany.

Hatami, M., M. C. M. Cuijpers and M. D. Boot (2015). Experimental optimization of the vanes geometry for a variable geometry turbocharger (VGT) using a Design of Experiment (DoE) approach. *Energy conversion and management* 106 (Supplement C), 1057-1070.

Huang, R., X. Luo, B. Ji, P. Wang, A. Yu, Z. Zhai and J. Zhou (2015). Multi-objective optimization of a mixed-flow pump impeller using modified NSGA-II algorithm. *Science China technological sciences* 58(12), 2122-2130.

Karassik, I. J. and J. T. McGuire (2012). *Centrifugal pumps*. Springer science & business media, Berlin, Germany.

Karassik, I. J., J. P. Messina, P. Cooper and C. C. Heald (2001). *Pump handbook*. McGraw-Hill, New York, US.

Kergourlay, G., M. Younsi, F. Bakir and R. Rey (2007). Influence of splitter blades on the flow

- field of a centrifugal pump: test-analysis comparison. *International Journal of Rotating Machinery* 2017, 1-13.
- Kim, S., Y. S. Choi, K. Y. Lee and J. H. Kim (2011). Design optimization of mixed-flow pump in a fixed meridional shape. *International journal of fluid machinery and systems* 4(1), 14-24.
- Korkmaz, E., M. Gölcü and C. Kurbanoğlu (2017). Effects of blade discharge angle, blade number and splitter blade length on deep well pump performance. *Journal of Applied Fluid Mechanics* 10(2), 529-540.
- Li, W. G. (2006). Analysis of flow in extreme low specific speed centrifugal pump impellers with multi-split-blade. *International Journal of Turbo and Jet Engines* 23(2), 73-86.
- Lian, Y. and M. S. Liou (2005). Multi objective optimization using coupled response surface model and evolutionary algorithm. *AIAA Journal* 43(6), 1316-1325.
- Memardefzouli, M., and A. Nourbakhsh (2009). Experimental investigation of slip factors in centrifugal pumps. *Experimental Thermal and Fluid Science* 33(5), 938-945.
- Miyamoto, H., Y. Nakashima and H. Ohba (1992). Effects of splitter blades on the flows and characteristics in centrifugal impellers. *JSME international journal. Fluids engineering, heat transfer, power, combustion, thermophysical properties* 35(2), 238-246.
- Mojaddam, M. and K. R. Pullen (2019). Optimization of a centrifugal compressor using the Design of Experiment technique. *Applied Sciences*, 9(2), 291-311.
- Mojaddam, M., A. Hajilouy Benisi and M. R. Movahhedy (2012, June). Investigation on effect of centrifugal compressor volute cross-section shape on performance and flow field. In *ASME Turbo Expo 2012: Turbine Technical Conference and Exposition*, Copenhagen, Denmark.
- Mojaddam, M., A. Hajilouy Benisi and M. R. Movahhedy (2015). Optimal design of the volute for a turbocharger radial flow compressor. *Proceedings of the Institution of Mechanical Engineers, Part G: Journal of Aerospace Engineering* 229(6), 993-1002.
- Mojaddam, M., and S. A. M. Torshizi (2017). Design and optimization of meridional profiles for the impeller of centrifugal compressors. *Journal of Mechanical Science and Technology* 31(10), 4853-4861.
- Montgomery, D. C. (2017). *Design, and analysis of experiments*. John Wiley & Sons Inc., Hoboken, US.
- Montgomery, D. C., G. C. Runger and N. F. Hubele (2009). *Engineering statistics*. John Wiley & Sons, Hoboken, US.
- Moussavi, S. A., A. H. Benisi and M. Durali (2017). Effect of splitter leading edge location on performance of an automotive turbocharger compressor. *Energy* 123(Mar), 511-520.
- Myers, R. H., D. C. Montgomery and C. M. Anderson-Cook (2016). *Response surface methodology: process and product optimization using designed experiments*. John Wiley & Sons, US.
- Nikparto, A. and M. T. Schobeiri (2017). Experimental investigation of film-cooling effectiveness of a highly loaded turbine blade under steady and periodic unsteady flow conditions. *Journal of Heat Transfer* 139(7), 072201.
- Nourbakhsh, A., A. Jaumotte, C. Hirsch and H. B. Parizi (2007). *Turbopumps and pumping systems*. Berlin, Germany.
- Pei, J., T. Yin, S. Yuan, W. Wang and J. Wang (2017). Cavitation optimization for a centrifugal pump impeller by using orthogonal design of experiment. *Chinese Journal of Mechanical Engineering* 30(1), 103-109.
- Pei, J., W. Wang and S. Yuan (2016). Multi-point optimization on meridional shape of a centrifugal pump impeller for performance improvement. *Journal of Mechanical Science and Technology* 30(11), 4949-4960.
- Safikhani, H., A. Khalkhali and M. Farajpoor (2011). Pareto based multi-objective optimization of centrifugal pumps using CFD, neural networks and genetic algorithms. *Engineering Applications of Computational Fluid Mechanics* 5(1), 37-48.
- Samad, A., K. Y. Kim, T. Goel, R. T. Haftka and W. Shyy (2008). Multiple surrogate modeling for axial compressor blade shape optimization. *Journal of Propulsion and Power* 24(2), 301-310.
- Shahpar, S. A. (2000, May). Comparative study of optimisation methods for aerodynamic design of turbomachinery blades. In *ASME Turbo Expo 2000: Power for Land, Sea, and Air*, Munich, Germany.
- Shigemitsu, T., J. Fukutomi, T. Wada and H. Shinohara (2013). Performance analysis of mini centrifugal pump with splitter blades. *Journal of Thermal Science* 22(6), 573-579.
- Suh, J. W., J. W. Kim, Y. S. Choi, J. H. Kim, W. G. Joo and K. Y. Lee (2017). Multi-objective optimization of the hydrodynamic performance of the second stage of a multi-phase pump. *Energies* 10(9), 1334.
- Talebian, M. and M. Mojaddam (2017, May). Centrifugal compressor diffuser optimization by the means of DoE methods and RSM, In *Proceedings of 25th Annual International Conference on Mechanical Engineering*, Tehran, Iran.

Wang, C., W. Shi, X. Wang, X Jiang, Y Yang, W Li and L. Zhou (2017). Optimal design of multistage centrifugal pump based on the combined energy loss model and computational fluid dynamics. *Applied Energy* 187(Feb.), 10-26.

Zhang, J. Y., S. J. Cai, Y. J. Li, Zhou X. and Y. Zhang (2017). Optimization design of multiphase pump impeller based on combined genetic algorithm and boundary vortex flux diagnosis. *Journal of Hydrodynamics, Ser. B* 29(6), 1023-1034.